ACS APPLIED MATERIALS & INTERFACES

Research Article

www.acsami.org

# Recovery of Dilute Aqueous Acetone, Butanol, and Ethanol with Immobilized Calixarene Cavities

Anthony B. Thompson, Rachel C. Scholes, and Justin M. Notestein*

Department of Chemical and Biological Engineering, Northwestern University, Technological Institute E136, 2145 Sheridan Road, Evanston, Illinois 60208-3120, United States

Supporting Information

**ABSTRACT:** Macrocyclic calixarene molecules were modified with functional groups of different polarities at the upper rim and subsequently grafted to mesoporous silica supports through a single Si atom linker. The resulting materials were characterized by thermogravimetric analysis, UV−visible spectroscopy, nitrogen physisorption, and solid-state NMR spectroscopy. Materials were then used to separate acetone, *n*-butanol, and ethanol from dilute aqueous solution, as may be useful in the recovery of fermentation-based biofuels. For the purpose of modeling batch adsorption isotherms, the materials were considered to have one strong adsorption site per calixarene molecule and a larger number of weak adsorption sites on the silica surface and external to the calixarene cavity. The magnitude of the net free energy change of adsorption varied from approximately 15 to 20 kJ/mol and was found to decrease as upper-rim calixarene functional groups became more electron-withdrawing. Adsorption appears to be driven by weak van der Waals interactions with the calixarene cavity and, particularly for butanol, minimizing contacts with solvent water. In addition to demonstrating potentially useful new sorbents, these materials provide some of the first experimental estimates of the energy of interaction between aqueous solutes and hydrophobic calixarenes, which have previously been inaccessible because of the insolubility of most nonionic calixarene species in water.

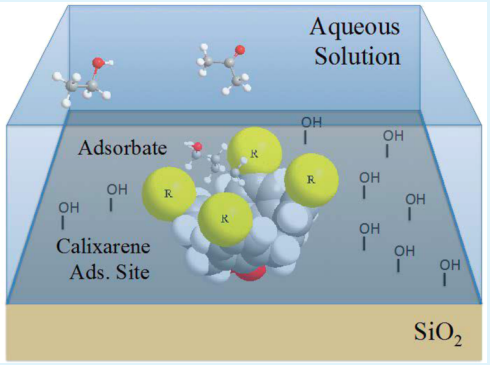


**KEYWORDS:** *adsorption, biofuels, calixarenes, silica, aqueous, fermentation*

## INTRODUCTION

The increasing cost of oil in recent years has led to a renewed interest in acetone−butanol−ethanol (ABE) fermentation for the production of *n*-butanol as an alternative fuel. Butanol has, for example, a higher energy density than ethanol, good mixing properties with other fuels, and a research octane number and energy content similar to those of gasoline.[1] Nevertheless, most butanol produced in the United States today is synthesized from oil, which is still the most cost-effective route.[2] A large fraction of the cost of ABE fermentation is due to the difficulty in separating the products from the dilute aqueous solution; for example, when traditional distillation is used, the energy consumption of the entire process has been known to exceed the energetic value of the product itself.[3] Maximum product concentrations are typically less than 0.25 M (19 g/L, or ∼0.5 mol %), as increasing yield beyond this point leads to cell death from cytotoxicity of butanol.[4] These low concentrations, along with the high boiling point of butanol, a heterogeneous azeotrope at 365 K,[5] and the presence of other compounds, make traditional distillation a costly recovery option. For these reasons, new and more cost-effective separation and recovery methods are needed for ABE fermentation to compete economically with crude oil.

Although the separation process is costly by way of distillation alone, past research has shown that preceding distillation by another step can significantly reduce the overall energy demand. For example, one study showed that in binary distillation of butanol from water, when the concentration of the feed was increased from 12 to 19 g/L (0.16 to 0.26 M), the energy demand of distillation was approximately halved; similarly, increasing the feed concentration from 10 to 40 g/L (0.13 to 0.54 M) reduced the ratio of energy input to energy content of the product from 1.5 to 0.25.[6] Thus, separations techniques capable of concentrating the products more efficiently than distillation could have a significant impact on the overall cost when used as a preceding step.

A wide variety of techniques are available, including in situ vacuum recovery,[7] gas stripping, supercritical extraction,[8] eutectic freeze crystallization, liquid−liquid extraction, and osmosis,[4] but pervaporation[9] and adsorption[3] are likely the best options available, with an estimated energy demand only ∼10% of the combustion enthalpy of *n*-butanol.[4] Within the category of adsorption, a great number of materials have been studied, including zeolites, activated carbons, ordered mesoporous or amorphous silicas, and polymers.[3,10] Furthermore, in the subcategory of materials based on silica, a very wide variety of

Received: September 24, 2013
Accepted: December 13, 2013
Published: December 13, 2013

   dx.doi.org/10.1021/am404182m | ACS Appl. Mater. Interfaces 2014, 6, 289−297

surface modifications are possible, giving a correspondingly wide range of associated properties.

Here, silica surfaces are modified by immobilized calixarenes, with each calixarene molecule intended to act as a single adsorption site. There is a wide literature basis on calixarene host−guest chemistry in solution, which provides a rationale for the design of specific adsorbents and may provide insight into the observed adsorption behavior on the molecular level. Additionally, calixarenes make up an extremely diverse class of molecules,[11] potentially enabling the fine-tuning of adsorption sites for highly specific materials.

We have previously investigated[12] the use of silica-immobilized calixarenes bearing hydrophobic groups at the upper rim to act as adsorption sites for butanol from dilute aqueous solution. Adsorption on these materials can be represented as the net process of exchanging solvent water molecules for an adsorbate molecule within the calixarene cavity.[13] With hydrophobic (Scheme 1, R = H or alkyl)

**Scheme 1. Immobilization of Calixarenes on Silica**[a]

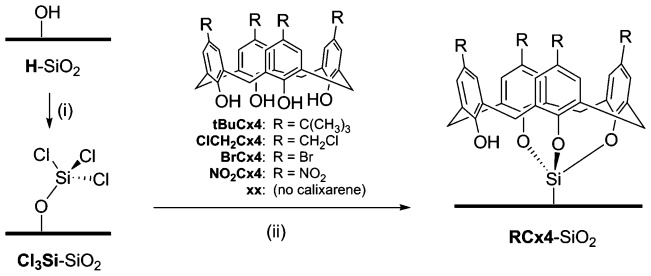


[a]Reaction conditions: (i) treat with 1:1 $SiCl_4$:$Et_3N$ in anhydrous $CH_2Cl_2$, RT, 24 h; (ii) reflux in anhydrous toluene, 24−48 h.

calixarenes, the net enthalpy change of adsorption of *n*-butanol is slightly more favorable than the theoretical phase separation from water into condensed butanol and increases with increasing molecular surface area of the calixarene cavity. This behavior is consistent with an adsorption process driven by weak intermolecular van der Waals forces and a net entropy increase likely associated with release of water molecules from the vicinity of the hydrophobic cavities.[12]

Here we continue investigating the use of rigidly grafted calixarenes as adsorption sites for aqueous separations, but the diversity of upper-rim functional groups is expanded to include strongly electron-withdrawing groups like $-NO_2$ or −Br to study the effect of polarizing the cavity. In spite of broad interest, the polarized calixarenes used here do not appear to have been previously immobilized onto a surface for use related to adsorption or separations. The adsorption of acetone and ethanol has also been studied, both for the relevance of these adsorbates to ABE adsorption and for their smaller size and potential for stronger dipole−dipole interactions with calixarene cavities. This will further our understanding of the host−guest interactions between water-soluble guests and highly hydrophobic calixarene molecules, where experimental data have not been previously available due to the insolubility of most nonionic calixarenes in water and the absence of suitably functionalized materials.

## EXPERIMENTAL METHODS

All glassware was stored in a drying oven at 120 °C prior to synthesis. The following procedures were carried out under a dry nitrogen atmosphere using standard air-free techniques. All water used in synthesis and experiments was filtered and deionized to 18.2 MΩ-cm resistivity.

**Synthesis.** Reagents used in precursor syntheses were obtained from Sigma-Aldrich, with the exception of $AlCl_3$, which was obtained from Alfa Aesar; all reagents were used as received. The starting material for all precursors was **tBuCx4** (95%, Sigma-Aldrich), which was used without further purification. Solvents were purified by distillation from $CaH_2$ or, in the case of DMF, by distillation from $MgSO_4$ under reduced pressure.[14] All calixarenes are known in the literature, and their identities and purities were confirmed by $^1H$ and $^{13}C$ NMR.

**HCx4** (R = H in Scheme 1) served as the intermediate for all other calixarenes and was synthesized by de-*tert*-butylation of **tBuCx4** using $AlCl_3$ and phenol following a previously published patent.[15] $^1H$ NMR ($CDCl_3$): 10.21 (s, 4H, OH), 7.06 (d, 8H, ArH(*m*)), 6.73 (t, 4H, ArH(*p*)), 4.26 (bs, 4H, $ArCH_2Ar$), 3.55 (bs, 4H, $ArCH_2Ar$). $^{13}C$ NMR ($CDCl_3$): 148.89 (C−OH), 129.11 (CH (*m*)), 128.36 (CH (*p*)), 122.39 ($\underline{C}-CH_2$), 31.84 ($CH_2$).

**$ClCH_2$Cx4** was synthesized by chloromethylation of **HCx4** with chloromethyl-*n*-octyl ether and $SnCl_4$ according to a published procedure.[16] $^1H$ NMR ($CDCl_3$): 10.13 (s, 4H, OH), 7.09 (s, 8H, ArH), 4.42 (s, 8H, $ArCH_2Cl$), 4.21 (bs, 4H, $ArCH_2Ar$), 3.55 (bs, 4H, $ArCH_2Ar$). $^{13}C$ NMR ($CDCl_3$): 149.00 (C−OH), 131.51 ($\underline{C}-CH_2Cl$), 129.63 (CH), 128.36 ($\underline{C}-CH_2Ar$), 45.97 ($ArCH_2Cl$), 29.86 ($ArCH_2Ar$).

**BrCx4** was synthesized from **HCx4** with $Br_2$ in DMF according to a previously published procedure.[17] $^1H$ NMR (DMSO-$d_6$): 7.32 (s, 8H, ArH), 3.79 (bs, 8H, $ArCH_2Ar$). $^{13}C$ NMR (DMSO-$d_6$): 151.47 (C−OH), 131.41 (CH), 130.69 ($\underline{C}-CH_2$), 110.61 (C−Br), 30.40 ($CH_2$).

**$NO_2$Cx4** was synthesized by sulfonation and subsequent nitration of **HCx4** with concentrated $H_2SO_4$ followed by dilute $HNO_3$ in the presence of $H_2SO_4$ according to a previously published procedure.[18] $^1H$ NMR (DMSO-$d_6$): 8.16 (s, 8H, ArH), 4.5−9.0 (bbs, 4H, OH), 4.25 (bs, 4H, $ArCH_2Ar$), 3.72 (bs, 4H, $ArCH_2Ar$). $^{13}C$ NMR (DMSO-$d_6$): 162.47 (C−OH), 138.17 ($C-NO_2$), 129.54 (CH), 124.72 ($\underline{C}-CH_2$), 30.58 ($CH_2$).

Mesoporous silica gel (Selecto Scientific) with a primary particle size of 100−200 μm, an approximate surface area of 500 $m^2/g$, and an average pore diameter of 60 Å was used as the support for all materials and was stored in a drying oven at 120 °C prior to use. Triethylamine and silicon tetrachloride solution were obtained from Sigma-Aldrich; the $SiCl_4$ solution was used without further purification, whereas $Et_3N$ was freshly distilled from $CaH_2$ before each use.[14] The silica (1.5−6.0 g) was first dried under dynamic vacuum of <50 mTorr at 250 °C for 12 h and then cooled to ambient temperature, and the flask was backfilled with $N_2$. $SiCl_4$ (1.0 M in $CH_2Cl_2$) was added (4.5 mL per gram of starting material), followed by dropwise addition of triethylamine (0.6 mL per gram of starting material) while shaking, which resulted in an exothermic reaction and an opaque suspension. After shaking for 12 h at room temperature, the solvent was removed in vacuo (20 min at ambient temperature or until no liquid was visible), and then the chlorinated $SiO_2$ was heated to 70 °C and evacuated for an additional 12 h to sublime off the generated triethylamine hydrochloride salt.

The calixarene (0.3 mmol per gram of starting material, in slight excess of the maximum surface density previously reported to be achievable by this method, which is approximately half a monolayer[19]) was then dissolved or partially dissolved in anhydrous toluene (10 mL per gram of starting material) at 100 °C; samples that only partially dissolved (**$NO_2$Cx4**, **BrCx4**) were then subjected to ultrasonics for 5−10 min to break up large particles. The chlorinated $SiO_2$ was then transferred to the calixarene solution under air-free conditions. For all calixarenes except **$ClCH_2$Cx4**, a small amount of triethylamine (1.1 mol per mole calix) was then added to trap generated acid, and the suspension was refluxed under $N_2$ for 24−72 h. Triethylamine had to be excluded in the case of **$ClCH_2$Cx4** materials, as the two compounds readily reacted to give a blue product, possibly a cyclohexadienone-type structure.[20] Instead, dry $N_2$ gas was periodically bubbled through the mixture to purge generated HCl vapor and drive the reaction forward.

Materials were then washed sequentially with (per 1 g of starting material) 100 mL of boiling toluene, 50 mL of methanol, 50 mL of water, 50 mL of methanol, 100 mL of acetonitrile, and 50 mL of petroleum

**Table 1. Results from Materials Characterization**

| | TGA[a] | | | UV−vis | | BET | |
|---|---|---|---|---|---|---|---|
| | $\sigma$ | $\rho_s$[b] | $w_{Cx}$ | $\lambda_{max}$[c] | $D_{pore}$ | $V_{pore}$ | $S_{BET}$ |
| material | mmol/$g_{matl}$ | $nm^{-2}$ | wt % | nm | Å | $cm^3/g_{matl}$ | $m^2/g_{matl}$ |
| **xx**-$SiO_2$ | 0.00 | 0.00 | 0.0 | -- | 56 | 0.76 | 540 |
| **tBuCx4**-$SiO_2$ | 0.11 | 0.14 | 7.7 | 284 | 58 | 0.74 | 510 |
| **ClCH$_2$Cx4**-$SiO_2$ | 0.20 | 0.28 | 14.0 | 287 | 43 | 0.54 | 510 |
| **BrCx4**-$SiO_2$ | 0.16 | 0.22 | 13.0 | 287 | 49 | 0.62 | 500 |
| **NO$_2$Cx4**-$SiO_2$ | 0.11 | 0.14 | 7.0 | 289 | 52 | 0.66 | 510 |

[a]All values ±10%. [b]Based on BET surface area of unmodified support, 500 $m^2/g$. [c]Wavelength of maximum pseudoabsorbance, corresponding to the calixarene aromatic peak.

ether. After briefly air-drying, the materials were Soxhlet or Gregar extracted with anhydrous toluene for 12 h and dried under dynamic vacuum at ambient temperature. Materials containing potentially hydrolyzable groups (**BrCx4** and **ClCH$_2$Cx4**) were washed extensively with water at ambient temperature, whereas all other materials were Soxhlet or Gregar extracted with water for 12 h. Finally, the materials were dried under dynamic vacuum at ambient temperature overnight, passed over a 63 $\mu$m sieve to remove fine particulates, and then passed through a 177 $\mu$m sieve to remove large debris. Materials were stored in a desiccator at ambient temperature.

**Characterization.** Thermogravimetric analysis (TGA) experiments were conducted on a TA Instruments TGA Q500 in high-resolution mode with a 10 °C/min ramp to 800 °C under a flow of dry synthetic air. Diffuse-reflectance UV−visible spectra were recorded on a Shimadzu UV-3600 spectrometer using a Harrick Praying Mantis accessory with PTFE powder as a perfect reflector standard. Nitrogen physisorption isotherms were recorded on a Micromeritics ASAP 2010 CE system at 77.4 K. Solution-phase proton and carbon-13 nuclear magnetic resonance ($^1$H and $^{13}$C NMR) spectra were recorded on a Bruker Avance III 500 MHz spectrometer equipped with a direct cryoprobe. Solid-state carbon-13 cross-polarization/magic angle spinning nuclear magnetic resonance ($^{13}$C CP-MAS NMR) spectra were recorded on a 400 MHz Varian spectrometer equipped with a 5 mm triple-resonance probe at a spin rate of 5 kHz.

**Adsorption.** All adsorption isotherms reported in this study are for a single species (acetone, butanol, or ethanol) in water. Batchwise adsorption experiments were conducted on a scale of 100 mg of material per 1 mL of binary solution at 20 ± 1 °C using a method previously described by the authors.[12] As during the synthesis step, light shaking is preferred to stirring to avoid mechanical grinding of the materials, which causes exposure of unmodified internal surfaces.[21] Final concentrations were determined by refractive index at 20 °C using an Atago RX-007$\alpha$ temperature-controlled benchtop refractometer, which was previously calibrated against binary aqueous acetone, *n*-butanol, and ethanol stock solutions of known concentrations. Experimental reproducibility of the equilibrium adsorbate concentrations was ±1.1 mM, 0.67 mM, and 1.8 mM for acetone, *n*-butanol, and ethanol, respectively, which corresponds to an approximate 5−10% uncertainty in uptake measurements (mol adsorbate per mol calix) for the dilute solutions used. Refractive index was measured at least twice for each sample. A small amount of uncertainty is introduced by desorption of impurities from the material, such as residual solvents from synthesis. This was kept to a minimum by the rigorous washing, extraction, and sieving steps mentioned previously.

The observed uptakes were considered to consist of adsorption into strong sites associated with the calixarene cavities as well as weaker adsorption onto the exposed silica surface and other possible adsorption sites on the calixarenes themselves but external to the cavity. The latter is hereafter referred to as the "background adsorption". The aim of data fitting is to separate properties specific to the calixarene cavities from the total uptake data. Given the relatively large uncertainties and batch-to-batch variability, the background adsorption was assumed proportional to the amount of adsorbate over the concentration range studied. Although a simplification, a Henry-type relationship[22] is not unreasonable in this case considering the low concentration range studied and that the nonspecific "background" adsorption is expected to be far from saturation or adsorption at the calixarene cavities; on the other hand, we expect a narrower distribution of adsorption energies and assume Langmuirian saturation behavior.[23] Furthermore, here it is assumed that the saturation amount of adsorbate, $\sigma$ (mmol/g), is equal to the number of grafted calixarenes as set by the synthesis conditions and determined from TGA. Together then, the total uptake is described by only two adjustable parameters, one of which is specific to the interactions with the calixarene cavity.

We then consider the total uptake $q$ (mmol/g) of solute $i$ (A, B, or E) to be a linear sum of the background adsorption $q_0$ and the adsorption to the calixarene cavities $q_c$; thus

$$q_i = q_{0_i} + q_{c_i} = k_0 x_i + \frac{\sigma K x_i}{1 + K x_i} \quad (1)$$

where

$$K \equiv \exp\left(\frac{-\Delta G_{net}}{RT}\right) \quad (2)$$

Dividing eq 1 by the calixarene loading $\sigma$

$$\theta = \frac{q}{\sigma} = k' x_i + \frac{K x_i}{1 + K x_i} \quad (3)$$

where

$$k' \equiv \frac{k_0}{\sigma} \quad (4)$$

In eqs 1−4, $k_0$ (mmol/g) is the Henry-like constant describing background adsorption; $x_i$ is the mole fraction of solute $i$ in water; $K$ is the (unitless) equilibrium constant for adsorption into the calixarene cavities; and $\Delta G_{net}$ (kJ/mol) is the net free energy change caused by adsorption of one mole of solute onto one mole of calixarene sites in water. Mole fractions were approximated from the known molarities by assuming the density of all solutions to be equal to the density of water. The fractional uptake $\theta$ is defined as the uptake of adsorbate molecules per calixarene cavity to allow for comparison across materials with different values of $\sigma$. Equation 3 is used for all adsorption data fitting in this study.

## RESULTS AND DISCUSSION

**Characterization.** Calixarene loadings given in Table 1 were calculated from TGA weight loss curves (Figures S1 and S2, Supporting Information) by assuming that all mass loss below 300 °C was due to vaporization of residual solvents from synthesis (mostly water), and the mass loss from 300 to 800 °C was due to combustion of calixarene fragments. Only a small mass loss was observed near 420 °C in the baseline material **xx**-$SiO_2$ indicating that combustion of surface methoxy groups and other species remaining after the workup contributed only negligibly. These species are present on all materials but have been minimized by the extensive washing, which, in particular,


dx.doi.org/10.1021/am404182m | ACS Appl. Mater. Interfaces 2014, 6, 289−297

should hydrolyze reactive groups[24] to form a new layer of silica around the calixarene cavities.

Figure 1 shows the solid-state $^{13}C$ CP-MAS NMR spectra for all materials. Despite the broadness of the peaks, it is observed

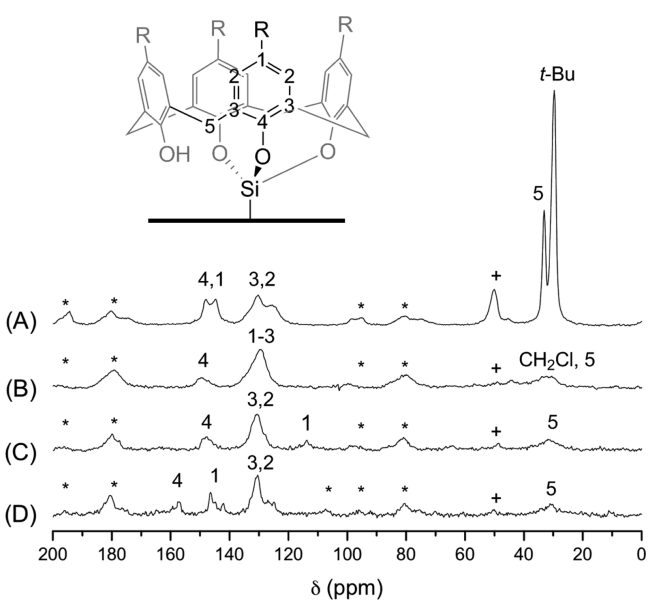


**Figure 1.** $^{13}C$ CP-MAS NMR spectrum of **tBuCx4** (A), **ClCH$_2$Cx4** (B), **BrCx4** (C), and **NO$_2$Cx4** (D) collected at a spin rate of 5 kHz. Spinning sideband peaks are denoted by *; surface methoxy species are denoted by +.

that the chemical shifts approximately correspond to those of the precursors in solution, listed in the Experimental Section and illustrated graphically in Figure S3 (Supporting Information). In the aromatic region, chemical shifts of carbons not attached to the R group are generally the same for all four materials. As expected, the resonance of carbon 1 differs significantly with the identity of the R group to which it is bound, generally shifting upfield as polarity increases but with a large downfield shift for R = $NO_2$. The difference in this chemical shift compared to the other materials is probably due to the strong electron-withdrawing effect of the nitro group, which results from both resonance and induction, whereas halides are electron-withdrawing via induction but electron-donating via resonance.[25] The feature at 30 ppm in (B)−(D) is from the methylene groups; in (A) this feature is obscured by the large *tert*-butyl peak. The peak at 50 ppm observed on all spectra is due to the surface methoxy species derived from solvent washings.

The diffuse-reflectance UV−visible pseudoabsorbance spectra are presented in Figure S4 (Supporting Information). All spectra show a peak near 287 nm, which corresponds to ultraviolet absorption by the aromatic calixarene subunits. This peak shifts to slightly higher wavelengths systematically as the electron-withdrawing character of the upper-rim group (e.g., Hammett *para* substituent constant) increases, as indicated in Table 1.

Nitrogen physisorption isotherms at 77.4 K (Figure S5, Supporting Information) were fit to the standard BET equation.[26] The BET surface area ($S_{BET}$) values for these materials are given in Table 1. The pore volumes at $P/P_0 = 0.99$ and average pore diameters of the materials, as determined by the BJH method,[27] decrease systematically with increasing loadings of calixarenes on the surface (Table 1). Pore size distributions (Figure S6, Supporting Information) are skewed toward smaller median diameters on the calixarene materials when compared to the control material **xx**-$SiO_2$ (Table 1). This effect is consistent with deposition of calixarenes on the pore walls, decreasing their mean diameter. Micropores intrinsic to the support are not altered by immobilization of the large calixarene molecules, indicating that the grafting procedure does not result in pore blocking of the material. It is also seen that the pore volumes decrease more significantly than do specific $N_2$-accessible surface areas. This result is consistent with an inverted cone conformation of the calixarene on the silica surface, which would occupy significant pore volume but only take up a small amount of the $SiO_2$ surface area. This result may also indicate that $N_2$ is adsorbed onto the hydrophobic surface of the calixarenes themselves, thus compensating for the loss in $SiO_2$ surface area due to grafting.

**Adsorption.** Previously, we showed that the strongest adsorption sites for a given material correlate linearly with the number of grafted calixarenes, reinforcing our claim that the calixarenes are the strong adsorption sites. Here, experimental fractional uptake ($\theta$) isotherms vs ABE mole fraction are given in Figures 2 and 3, which show the same data arranged differently for more facile comparisons. The former compares materials for a given adsorbate, whereas the latter compares the different adsorbates for a given material. Figure S9 in the Supporting Information also gives uptake data normalized by adsorbent mass, for more direct comparison with conventional adsorbent materials. Figure 2 shows that the most nonpolar calixarene, with *tert*-butyl R groups, has the greatest uptake for all three adsorbates. Also for all adsorbates, the fitted uptake with respect to the R group follows the order *t*-Bu > $ClCH_2$ > Br > $NO_2$. Figure 3 shows that for all four materials the total uptake follows the order acetone > *n*-butanol > ethanol at a given equilibrium concentration.

Table 2 shows the fitting parameters $k'$ and $K$, as well as $\Delta G_{net}$ calculated directly from $K$ for adsorption at the calixarene sites. As $x \rightarrow 0$, the relative values of $K$ and $k'$ determine which process dominates the observed uptake; thus, it can be seen that the calixarene adsorption sites are always fitted as responsible for >65% of the uptake. The contribution is smallest for acetone, with other species adsorbing much more specifically to the calixarene sites. Consistent with total uptake shown in Figures 2 and 3, $K$ decreases in the order *t*-Bu > $ClCH_2$ > Br > $NO_2$ for all adsorbates. The nonspecific $k'$ decreases in the same order with few exceptions, indicating that the calixarene molecules do also alter the linear contribution to the adsorption isotherm for a given material. Expressed as $\Delta G_{net}$, the calixarene site adsorption becomes monotonically less favorable by ~3 kJ/mol, a statistically significant change (nonoverlapping uncertainties in $K$ and $p$-values <0.05, see Supporting Information Table S2), in moving down Table 2 from *t*-Bu to $NO_2$. In contrast, when comparing across adsorbates for a given material, $K$ of the calixarene sites is fit to values with no statistical difference in most cases (overlapping uncertainties in $K$ and $p$-values >0.05, see Supporting Information Table S2). Thus, when comparing the net adsorption of acetone, butanol, or ethanol from solutions of comparable mole fraction, much of the difference appears to come from the linear contribution to the isotherm associated with the calixarene exterior and residual silica surface, rather than the saturating contribution assigned to the interior of the calixarene cavity.

Although previous studies with water-soluble calixarenes have shown stronger net interactions for guests with more hydrophobic surface area,[28−31] more acidic C−H bonds on the guest


dx.doi.org/10.1021/am404182m | ACS Appl. Mater. Interfaces 2014, 6, 289−297

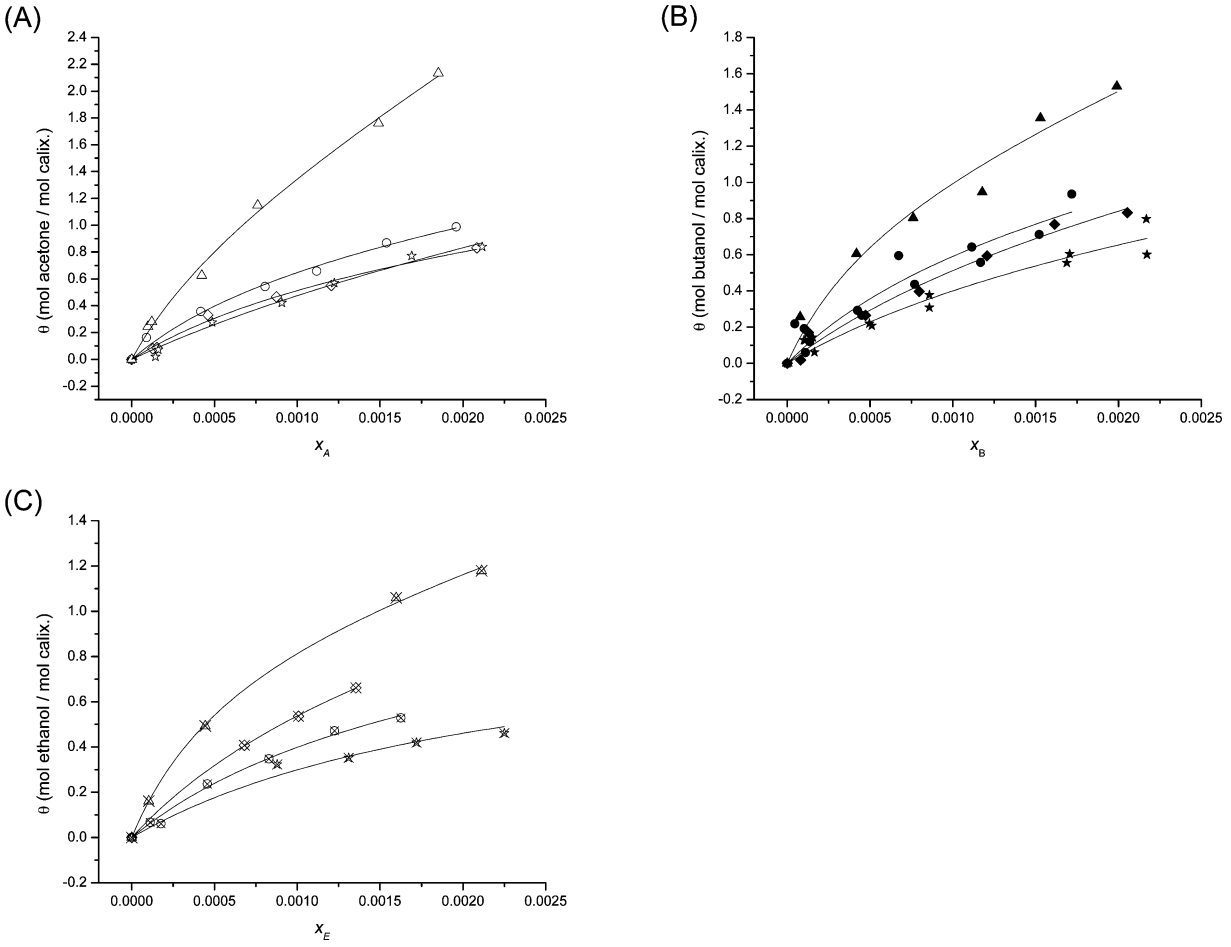


**Figure 2.** Adsorption isotherms for acetone (A), *n*-butanol (B), and ethanol (C) on materials containing **tBuCx4** (triangles), **ClCH$_2$Cx4** (circles), **BrCx4** (diamonds), and **NO$_2$Cx4** (stars).

have also been correlated to stronger interactions.[32] Thus, the similarities in fitted $K$ for different adsorbates may reflect a balance of competing properties.

In general, it is known[33] that solubility of the adsorbate can have a significant effect on liquid-phase adsorption isotherms, and much of the theory of adsorption from miscible solutions,[34] such as aqueous acetone or ethanol, is incompatible with the theory of adsorption from partially soluble mixtures[35] such as aqueous *n*-butanol. Although it is convenient to compare isotherms for this system based on mole fraction, their analysis is obscured by large differences in solubility of the analytes. Thus, it is necessary to deconvolute the net adsorption energy $\Delta G_{net}$ into its different contributions. Adsorption on these materials is described by a Born−Haber cycle (Figure 4) for host−guest chemistry involving (1) desorption of water from the cavity into a virtual vapor phase, $-\Delta G_{ads,w}$, (2) recondensation of water into solution, $-\Delta G_{vap,w}$, (3) vaporization of a guest molecule from solution, $-\Delta G_{sol,i}$, and (4) virtual vapor-phase adsorption of the guest to the cavity, $\Delta G_{ads,i}$. The total net adsorption energy is thus

$$\Delta G_{net} = -\Delta G_{ads,w} - \Delta G_{vap,w} - \Delta G_{sol,i} + \Delta G_{ads,i} \quad (5)$$

This analysis follows a similar scheme in a previous study by some of the authors.[13] This scheme simplifies the net adsorption process by assuming that the solvation of the calixarene−adsorbate complex cancels the desolvation of the calixarene−water complex shown in Figure 4.

We also assume infinite-dilution behavior since the solute concentration is very low ($x_i$ < 0.0025). The free energy of vaporization of water at 298 K is $\Delta G_{vap,w}$ = 8.6 kJ/mol,[36] and the free energy of solvation of solute i is the free energy of mixing pure solute into water less the free energy of vaporization; thus, $\Delta G_{sol,i} = RT \ln \gamma_i^{\infty} - \Delta G_{vap,i}$,[37] where $\Delta G_{vap,i}$ is the free energy of vaporization of the solute at 298 K ($\Delta G_{vap,B}$ = 2.8 kJ/mol, $\Delta G_{vap,A}$ = 3.0 kJ/mol, and $\Delta G_{vap,E}$ = 5.8 kJ/mol for *n*-butanol, acetone, and ethanol, respectively[38]) and $\gamma_i^{\infty}$ is the infinite-dilution activity coefficient of solute i in water at 298 K ($\gamma_B^{\infty}$ = 51.2, $\gamma_A^{\infty}$ = 7.68, and $\gamma_E^{\infty}$ = 3.91 for *n*-butanol,[39,40] acetone,[41] and ethanol,[40] respectively). The activity coefficients were calculated from correlations of compiled data in the cited reviews. Finally, the value of $\Delta G_{ads,w}$ is unknown, except for that of **tBuCx4**, as estimated from a prior study by some of the authors.[13] Thus, we define a free energy of adsorption of analyte i from the virtual vapor phase to the calixarene site, relative to that of water, as $\Delta\Delta G_i = \Delta G_{ads,i} - \Delta G_{ads,w}$. Overall, therefore

$$\Delta\Delta G_i = \Delta G_{net} + \Delta G_{vap,w} + RT \ln \gamma_i^{\infty} - \Delta G_{vap,i} \quad (6)$$

The values of $\Delta\Delta G_i$ calculated from eq 6 are given in Table 3. It is observed that adsorption of these small organic molecules from the virtual gas phase to a calixarene site is generally more favorable than that of water vapor, reflecting the highly hydrophobic nature of the adsorption sites. This free energy difference is approximately 9−12 kJ/mol for ethanol and 4−7 kJ/mol for acetone but only 0−3 kJ/mol for *n*-butanol, with an


dx.doi.org/10.1021/am404182m | ACS Appl. Mater. Interfaces 2014, 6, 289−297

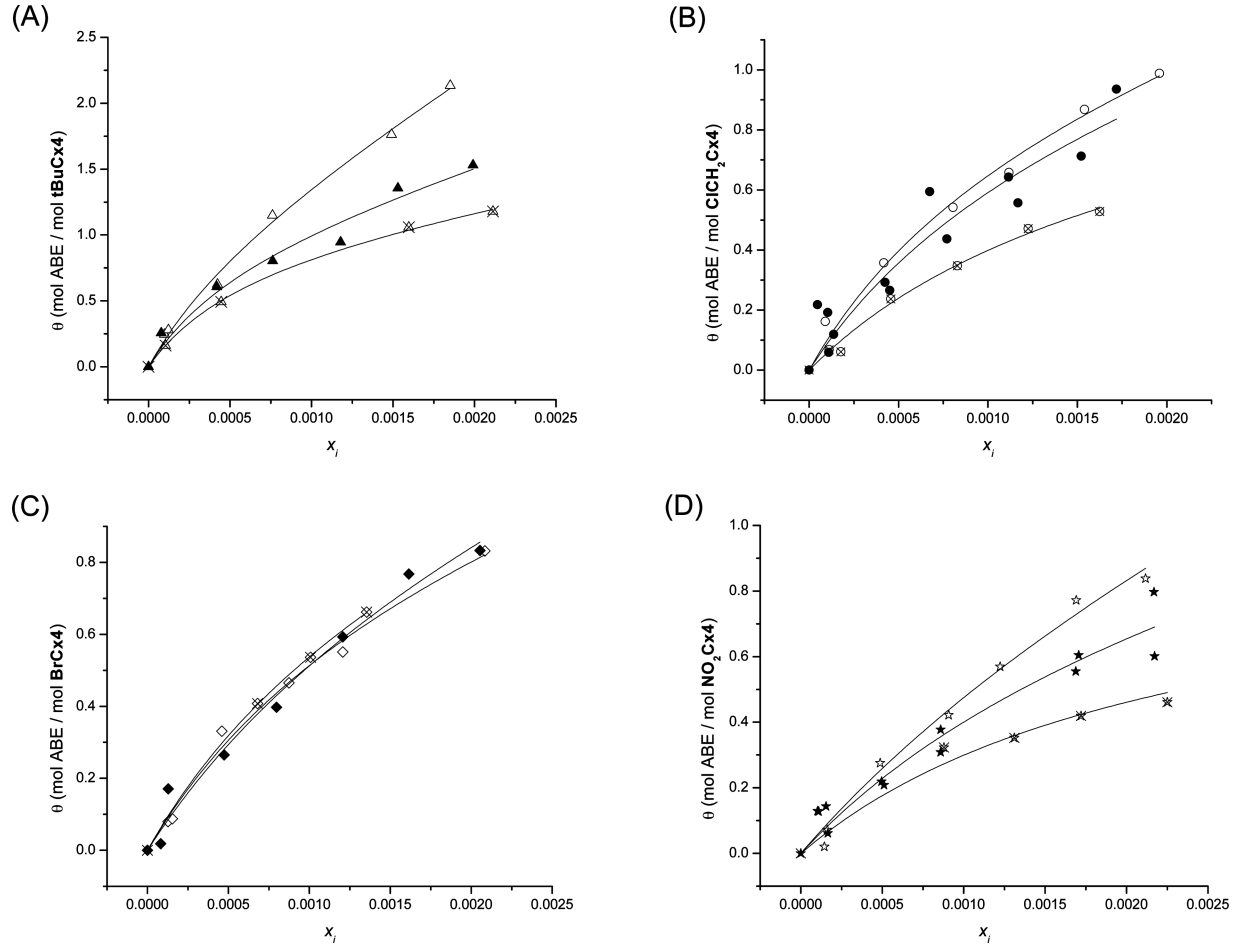


**Figure 3.** Adsorption isotherms for acetone (open symbols), *n*-butanol (solid symbols), and ethanol (crossed symbols) on materials containing **tBuCx4** (A), **ClCH$_2$Cx4** (B), **BrCx4** (C), and **NO$_2$Cx4** (D).

**Table 2. Values Obtained from Fitting Equation 3 to the Experimental Uptake Data for (B)utanol, (A)cetone, and (E)thanol**

| | $k'$ | | | $K$ | | | $\Delta G_{net}$ (kJ/mol) | | |
|---|---|---|---|---|---|---|---|---|---|
| material | B | A | E | B | A | E | B | A | E |
| **xx**-SiO$_2$ | 23 ± 2[a] | 53 ± 2[a] | 44 ± 4[a] | - | - | - | - | - | - |
| **tBuCx4**-SiO$_2$ | 360 ± 50 | 750 ± 40 | 200 ± 10 | 1690 ± 560 | 1510 ± 280 | 1570 ± 110 | −18.4 ± 1.0 | −18.2 ± 0.5 | −18.2 ± 0.2 |
| **ClCH$_2$Cx4**-SiO$_2$ | 150 ± 100 | 180 ± 30 | 40 ± 30 | 770 ± 310 | 900 ± 160 | 570 ± 90 | −16.5 ± 1.2 | −16.9 ± 0.5 | −15.7 ± 0.4 |
| **BrCx4**-SiO$_2$ | 150 ± 50 | 120 ± 20 | 140 ± 10 | 560 ± 150 | 660 ± 90 | 670 ± 30 | −15.7 ± 0.8 | −16.1 ± 0.4 | −16.1 ± 0.1 |
| **NO$_2$Cx4**-SiO$_2$ | 100 ± 50 | 200 ± 50 | 0 ± 0 | 460 ± 150 | 380 ± 120 | 430 ± 30 | −15.2 ± 0.9 | −14.8 ± 0.9 | −15.0 ± 0.2 |

[a] $k_0$ value in mmol/g from eq 1 with $\sigma = 0$. Note that $k'$ and $K$ are unitless.

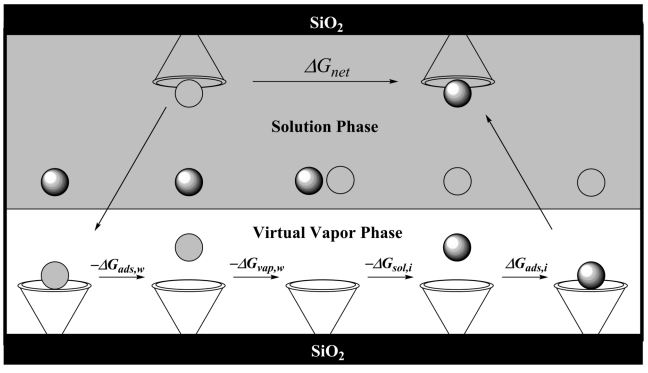


**Figure 4.** Born−Haber thermodynamic cycle for liquid-phase adsorption on calixarene−silica materials. Dark spheres represent adsorbate molecules, and light gray shading represents solvent water.

uncertainty of ∼1 kJ/mol, indicating that butanol adsorption from the gas phase is only slightly more favorable than that of water. Considering the dielectric constant $\varepsilon_i$ as a measure of the adsorbate's polarity ($\varepsilon_B$ = 17.8, $\varepsilon_A$ = 21.0, $\varepsilon_E$ = 25.3),[5] these adsorption sites preferentially bind the more polar adsorbates from the virtual vapor phase. A similar overall trend was observed by others in a study on the complexation of **NO$_2$Cx4** with *p*-substituted phenols in organic solvents; it was reported that *p*-nitrophenol formed the most stable complexes with the calixarene, while *p*-alkylphenol complexes were the least stable.[42]

In a previous study[13] the free energy of water removal from the cavity of **tBuCx4** was estimated as $\Delta G_{ads,w} = -16.6$ kJ/mol. Using this value along with the $\Delta\Delta G_i$ values for **tBuCx4** in Table 3, the free energies of adsorption from the virtual vapor phase ($\Delta G_{ads,i}$) to **tBuCx4** are approximately −19, −24, and −29 kJ/mol for *n*-butanol, acetone, and ethanol, respectively. A previous study by


dx.doi.org/10.1021/am404182m | ACS Appl. Mater. Interfaces 2014, 6, 289−297

some of the authors[13] showed free energies of gas-phase adsorption of small aromatic hydrocarbons (benzene, toluene, and xylenes; $\varepsilon \sim 2.3$) to be −13.5 to −14 kJ/mol, further consistent with our observation that adsorption is stronger with the more polar adsorbates.

**Table 3. Relative Free Energy of Adsorption of (B)utanol, (A)cetone, and (E)thanol from the Virtual Vapor Phase to Calixarenes**

| | | $\Delta\Delta G_i$ (kJ/mol) | | |
|---|---|---|---|---|
| calixarene | $\sigma^{*a}$ | B | A | E |
| **tBuCx4** | −0.197[b] | −2.8 ± 1.0 | −7.5 ± 0.5 | −12.0 ± 0.2 |
| **ClCH$_2$Cx4** | 0.120[c] | −0.9 ± 1.2 | −6.2 ± 0.5 | −9.5 ± 0.4 |
| **BrCx4** | 0.232[b] | −0.1 ± 0.8 | −5.4 ± 0.4 | −9.9 ± 0.1 |
| **NO$_2$Cx4** | 0.778[b] | +0.4 ± 0.9 | −4.1 ± 0.9 | −8.8 ± 0.2 |

[a]Hammett *para* substituent constant for the R group. [b]Literature values.[43] [c]Literature values.[44]

Although these materials preclude the use of solution-state NMR from which other investigators have deduced the structure of host−guest complexes,[29,45] we speculate that ethanol and butanol likely insert their alkyl chains into the calixarene cavities. This conformation would allow their hydroxyl groups to interact with solvent water via hydrogen bonding while allowing their hydrophobic tails to desolvate from water. Indeed, a recent molecular dynamics study found that *n*-alkanols from ethanol to heptanol formed inclusion complexes with *p*-sulfonatocalix[4]-arene in water at 25 °C. In each instance, the alkyl chain was inserted into the cavity, and the hydroxyl group was interacting with water molecules, which bridged the alcohol OH group to the calixarene's sulfonate groups. The authors concluded that the complexes were controlled by van der Waals interactions, as the Lennard-Jones dispersion energies were more than an order of magnitude higher than electrostatic energies. These van der Waals forces compensated for the unfavorable partial desolvation of the host and guest during complexation.[46] These results confirm an earlier study, also using *p*-sulfonatocalix[4]arenes, in which the enthalpy and entropy of complexation were determined via microcalorimetry; it was concluded that only alkyl residues are included into the cavity.[47]

Previous studies on water-soluble calixarenes have shown that more hydrophobic surface area on the host leads to a stronger overall interaction,[48] consistent with our observation that **tBuCx4** was the strongest adsorption site. In a previous study,[12] we showed a correlation between molecular surface area and adsorption strength for alkylcalixarenes. To develop an analogous quantitative relationship between calixarene polarity and adsorption strength, we use Hammett constants, which were originally developed to correlate reaction equilibrium constants for differently functionalized aromatic compounds,[49] but they have also been used to describe properties of immobilized calixarenes.[19] Table 3 lists the Hammett constants ($\sigma^*$) for the calixarene functional groups used in this study along with the calculated $\Delta\Delta G_i$, and Figure 5 shows the linear correlations between the energies and $\sigma^*$. For all three solutes considered here, $\Delta\Delta G_i$ decreases in magnitude by about 3 kJ/mol as the adsorption site becomes more electron-withdrawing (larger $\sigma^*$). Recalling that $\Delta\Delta G_i$ is a relative quantity, this observation could be due either to differences in adsorbate−calixarene interactions or to differences in the energetic penalty of removing water from the calixarene cavities.

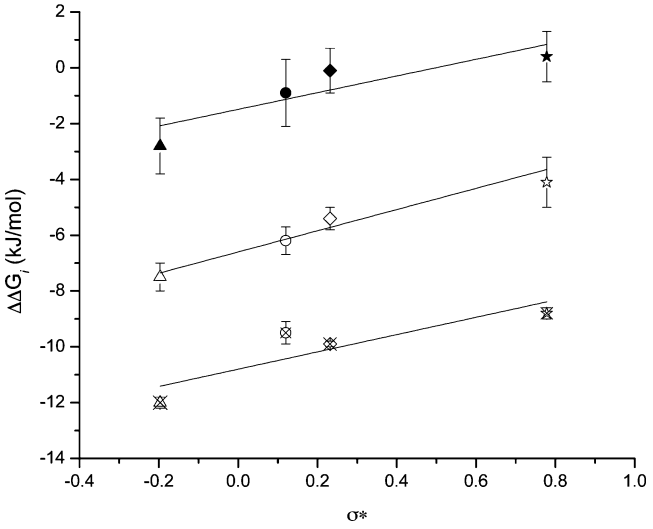


**Figure 5.** Relative adsorption free energy of *n*-butanol (solid symbols), acetone (open symbols), and ethanol (crossed symbols) as a function of the Hammett constant (*para*) of the R substituent. Solid lines are calculated by least-squares linear regression weighted by the inverse of the error values.

The similar slope in Figure 5 for all solutes suggests that the dependence of the relative adsorption energy, $\Delta\Delta G_i$, on the calixarene structure is driven by the water removal terms, $-\Delta G_{ads,w}$, since they are shared across all three solutes. Numerous computational studies have shown that cavity dehydration may be the most important driving force behind host−guest complexation processes in water.[50−53] Furthermore, tetrasulfonated calix[4]arenes are known to bind water into the cavity via the $\pi$ electron system of the phenolic cavity walls.[54] Thus, more electron-withdrawing upper-rim functional groups may lead to stronger interactions with water molecules, either through dipole−dipole attraction or OH−$\pi$ bonds. If this effect is more significant than analogous changes to the interactions with the solute, it would be consistent with the overall decreased uptake into calixarenes with electron-withdrawing groups. More strongly interacting calixarenes therefore have the seemingly counterintuitive effect of decreased net adsorption of acetone, butanol, or ethanol from water.

## CONCLUSIONS

Silica-supported calixarenes have been demonstrated as potential adsorbents for aqueous organics as applicable to biofuel separations from dilute aqueous fermentation broth. Because of the sterically enforced open conformation of the calixarene cavities and their highly dispersed nature on the hydrophilic support, calixarenes, which are by themselves insoluble in water without significant, property-changing modifications, are forcibly hydrated. This allows us to study calixarenes in water without adding solubilizing groups such as sulfonates or carboxylates, a subject for which essentially no data are available.

Materials have been characterized by TGA, UV−visible spectroscopy, and solid-state NMR, all of which are consistent with rigidly immobilized, intact calixarenes. $N_2$ physisorption experiments have shown that grafted calixarenes do not block micropores already present on the support and, despite occupying a significant fraction of the pore volume, do not reduce the total $N_2$ physisorption surface area, consistent with submonolayer grafting in a cone configuration.

Through batchwise adsorption experiments, it has been demonstrated that increasing the electron-withdrawing nature of upper-rim functional groups (quantified by Hammett substituent constants) leads to a small decrease in the magnitude of the net adsorption energy for acetone, *n*-butanol, and ethanol from aqueous solution, which has the practical effect of decreasing the adsorbent's capacity at a given solute concentration. At a given concentration, solutes are adsorbed in the order A > B > E, but differences in the equilibrium adsorption constant assigned to the adsorbate−calixarene interaction are not statistically significant. At a given activity (virtual vapor pressure), on the other hand, solutes would be preferentially adsorbed in the order E > A > B. In particular, the uptake of butanol at a given concentration is largely driven by its lower solubility in water. For butanol, adsorption onto all the calixarene cavities seems to be driven by desolvation of the molecule and general van der Waals interactions with the calixarene, as argued earlier.[12] The more polarized cavities can lead to energy penalties for the removal of more strongly bound water from within the cavity. As a result, butanol seems to preferentially adsorb to sites where there is a large hydrophobic surface area (i.e., **tBuCx4**).

These results help clarify the nature of interactions between hydrophobic calixarene cavities and guests in water, which are otherwise challenging to study. These findings also drive efforts to immobilize more diverse host molecules more able to balance the relative strengths of solvent and guest interactions.

## ■ ASSOCIATED CONTENT

### Ⓢ Supporting Information

Solution-state $^{13}C$ NMR spectra of synthesized calixarene precursors; thermogravimetric analysis; UV−visible spectra; $N_2$ physisorption; absolute adsorption isotherms (in mmol/g) for **xx**-$SiO_2$; table of $k'$ and $K$ values on an activity basis and a listing of statistical significance tests; adsorption data expressed in other units, for reference. This material is available free of charge via the Internet at http://pubs.acs.org.

## ■ AUTHOR INFORMATION

### Corresponding Author

*E-mail: j-notestein@northwestern.edu.

### Notes

The authors declare no competing financial interest.

## ■ ACKNOWLEDGMENTS

This work was funded by a grant from the National Science Foundation Division of Chemical, Bioengineering, Environmental, and Transport Systems (NSF CBET-0933667). All NMR data were recorded at the Integrated Molecular Structure Education and Research Center (IMSERC) at Northwestern University, which is supported by a grant from the National Science Foundation Division of Materials Research (NSF DMR-0521267) and by funding from Northwestern University.

## ■ REFERENCES

(1) Dürre, P. *Biotechnol. J.* **2007**, *2*, 1525−1534.
(2) Ramey, D.; Yang, S. *Energy, U.S.D.o.*, Ed. Morgantown, WV, 2004.
(3) Qureshi, N.; Hughes, S.; Maddox, I. S.; Cotta, M. A. *Bioprocess Biosyst. Eng.* **2005**, *27*, 215−222.
(4) Oudshoorn, A.; van der Wielen, L. A. M.; Straathof, A. J. J. *Ind. Eng. Chem. Res.* **2009**, *48*, 7325−7336.
(5) Haynes, W. M., Ed. *CRC Handbook of Chemistry and Physics*, 93rd Edition; CRC Press/Taylor and Francis: Boca Raton, FL, 2012.
(6) Philips, J. A.; Humphrey, A. E. An Overview of Process Technology for the Production of Liquid Fuels and Chemical Feedstocks via Fermentation. In *Organic Chemicals From Biomass*; Wise, D. L., Ed.; Benjamin/Cummings: Menlo Park, CA, 1983.
(7) Mariano, A. P.; Filho, R. M.; Ezeji, T. C. *Renewable Energy* **2012**, *47*, 183−187.
(8) Groot, W. J.; van der Lans, R. G. J. M.; Luyben, K. C. A. M. *Process Biochem.* **1992**, *27*, 61−75.
(9) Feng, X. S.; Huang, R. Y. M. *Ind. Eng. Chem. Res.* **1997**, *36*, 1048−1066.
(10) Nielsen, D. R.; Prather, K. J. *Biotechnol. Bioeng.* **2009**, *102*, 811−821.
(11) Böhmer, V. *Angew. Chem., Int. Ed.* **1995**, *34*, 713−745.
(12) Thompson, A. B.; Cope, S. J.; Swift, T. D.; Notestein, J. M. *Langmuir* **2011**, *27*, 11990−11998.
(13) Notestein, J. M.; Katz, A.; Iglesia, E. *Langmuir* **2006**, *22*, 4004−4014.
(14) Armarego, W. L. F.; Chai, C. L. L. *Purification of Laboratory Chemicals*; Elsevier: New York, 2003.
(15) Mayo, K. H.; Hoye, T. R.; Chen, X. *Calixarene-Based Peptide Conformation Mimetics, Methods of Use, and Methods of Making*. WO/2006/042104, 2006.
(16) Almi, M.; Arduini, A.; Casnati, A.; Pochini, A.; Ungaro, R. *Tetrahedron* **1989**, *45*, 2177−2182.
(17) Clark, T. E.; Makha, M.; Sobolev, A. N.; Rohrs, H.; Atwood, J. L.; Raston, C. L. *Chem.—Eur. J.* **2008**, *14*, 3931−3938.
(18) Shinkai, S.; Araki, K.; Tsubaki, T.; Arimura, T.; Manabe, O. *J. Chem. Soc., Perkin Trans. 1* **1987**, 2297−2299.
(19) Notestein, J. M.; Iglesia, E.; Katz, A. *Chem. Mater.* **2007**, *19*, 4998−5005.
(20) Volod'kin, A. A.; Ershov, V. V. *Russ. Chem. Bull.* **1962**, *11*, 317−320.
(21) Galbraith, J. W.; Giles, C. H.; Halliday, A. G.; Hassan, A. S. A.; McAllister, D. C.; Macaulay, N.; Macmillan, N. W. *J. Appl. Chem.* **1958**, *8*, 416−424.
(22) Henry, W. *Philos. Trans. R. Soc. London* **1803**, *93*, 29−274.
(23) Langmuir, I. *J. Am. Chem. Soc.* **1916**, *38*, 2221−2295.
(24) Bernards, T. N. M.; van Bommel, M. J.; Boonstra, A. H. *J. Non-Cryst. Solids* **1991**, *134*, 1−13.
(25) Hammett, L. P. *J. Am. Chem. Soc.* **1937**, *59*, 96−103.
(26) Brunauer, S.; Emmett, P. H.; Teller, E. *J. Am. Chem. Soc.* **1938**, *60*, 309.
(27) Barrett, E. P.; Joyner, L. G.; Halenda, P. P. *J. Am. Chem. Soc.* **1951**, *73*, 373−380.
(28) Nimse, S. B.; Kim, J.; Song, K.-S.; Kim, J.; Lee, J. T.; Nguyen, V.-T.; Ta, V.-T.; Kim, T. *Tetrahedron Lett.* **2011**, *52*, 3751−3755.
(29) Nimse, S. B.; Kim, J.; Ta, V.-T.; Kim, H.-S.; Song, K.-S.; Jung, C.-Y.; Nguyen, V.-T.; Kim, T. *Tetrahedron Lett.* **2009**, *50*, 7346−7350.
(30) Nimse, S. B.; Nguyen, V.-T.; Kim, J.; Kim, H.-S.; Song, K.-S.; Eoum, W.-Y.; Jung, C.-Y.; Ta, V.-T.; Seelam, S. R.; Kim, T. *Tetrahedron Lett.* **2010**, *51*, 2840−2845.
(31) Nimse, S. B.; Song, K.-S.; Kim, J.; Kim, H.-S.; Nguyen, V.-T.; Eoum, W.-Y.; Jung, C.-Y.; Ta, V.-T.; Kim, T. *Tetrahedron Lett.* **2010**, *51*, 6156−6160.
(32) Arduini, A.; Pochini, A.; Secchi, A.; Ugozzoli, F. Recognition of Neutral Molecules. In *Calixarenes*; Asfari, Z., Böhmer, V., Harrowfield, J., Vicens, J., Eds.; Kluwer Academic Publishers: Dordrecht, The Netherlands, 2001.
(33) Dabrowski, A.; Jaroniec, M.; Oscik, J., Multilayer and Monolayer Adsorption from Liquid Mixtures of Nonelectrolytes on Solid Surfaces. In *Surface and Colloid Science*; Matijevic, E., Ed.; Plenum Press: New York, NY, 1987; Vol. *14*, pp 83−213.
(34) Kipling, J. J. Adsorption from Completely Miscible Liquids. In *Adsorption from Solutions of Non-Electrolytes*; Academic Press Inc.: London, 1965; Chapter 4, pp 32−69.
(35) Kipling, J. J. Adsorption from Partially Miscible Liquids. In *Adsorption from Solutions of Non-Electrolytes*; Academic Press Inc.: London, 1965; Chapter 5, pp 70−85.
(36) Chase, M. W., Jr. *J. Phys. Chem. Ref. Data* **1998**, *9*, 1−1951.

(37) Sandler, S. I. *Chemical, Biochemical, and Engineering Thermodynamics*, 4th ed.; Wiley: New York, 2006.
(38) Linstrom, P. J., Mallard, W. G., Eds. *NIST Chemistry WebBook, NIST Standard Reference Database Number 69*; National Institute of Standards and Technology: Gaithersburg, MD.
(39) Hovorka, S.; Dohnal, V.; Roux, A. H.; Roux-Desgranges, G. *Fluid Phase Equilib.* **2002**, *201*, 135−164.
(40) Vrbka, P.; Fenclová, D.; Laštovka, V.; Dohnal, V. *Fluid Phase Equilib.* **2005**, *237*, 123−129.
(41) Kojima, K.; Zhang, S.; Hiaki, T. *Fluid Phase Equilib.* **1997**, *131*, 145−179.
(42) Kunsági-Máté, S.; Csók, Z.; Tuzi, A.; Kollár, L. *J. Phys. Chem. B* **2008**, *112*, 11743−11749.
(43) McDaniel, D. H.; Brown, H. C. *J. Org. Chem.* **1958**, *23*, 420−427.
(44) Hansch, C.; Leo, A. J. *Substituent Constants for Correlation Analysis in Chemistry and Biology*; Wiley-Interscience: New York, NY, 1979.
(45) Rehm, M.; Frank, M.; Schatz, J. r. *Tetrahedron Lett.* **2009**, *50*, 93−96.
(46) Ghoufi, A.; Morel, J. P.; Morel-Desrosiers, N.; Malfreyt, P. *J. Phys. Chem. B* **2005**, *109*, 23579−23587.
(47) Perret, F.; Morel, J. P.; Morel-Desrosiers, N. *Supramol. Chem.* **2003**, *15*, 199−206.
(48) Nimse, S. B.; Song, K.-S.; Kim, T. Water-Soluble Calix[4]arene Derivatives: Binding Stoichiometry and Spectroscopic Evaluation of the Host-Guest Recognition Mechanism. In *Stoichiometry and Research - The Importance of Quantity in Biomedicine*; Innocenti, A., Ed.; InTech: Rijeka, Croatia, 2012; pp 27−44.
(49) Hammett, L. P. *Chem. Rev.* **1935**, *17*, 125−136.
(50) Rogers, K. E.; Ortiz-Sanchez, J. M.; Baron, R.; Fajer, M.; de Oliveira, C. A. F.; McCammon, J. A. *J. Chem. Theory Comput.* **2013**, *9*, 46−53.
(51) Setny, P.; Baron, R.; McCammon, J. A. *J. Chem. Theory Comput.* **2010**, *6*, 2866−2871.
(52) Baron, R.; Setny, P.; McCammon, J. A. *J. Am. Chem. Soc.* **2010**, *132*, 12091−12097.
(53) Hummer, G. *Nature Chem.* **2010**, *2*, 906−907.
(54) Atwood, J. L.; Hamada, F.; Robinson, K. D.; Orr, G. W.; Vincent, R. L. *Nature* **1991**, *349*, 683−684.